

Provided for non-commercial research and education use.
Not for reproduction, distribution or commercial use.



This article was published in an Elsevier journal. The attached copy is furnished to the author for non-commercial research and education use, including for instruction at the author's institution, sharing with colleagues and providing to institution administration.

Other uses, including reproduction and distribution, or selling or licensing copies, or posting to personal, institutional or third party websites are prohibited.

In most cases authors are permitted to post their version of the article (e.g. in Word or Tex form) to their personal website or institutional repository. Authors requiring further information regarding Elsevier's archiving and manuscript policies are encouraged to visit:

<http://www.elsevier.com/copyright>



Molecules and solids in planetary nebulae and proto-planetary nebulae

Sun Kwok

Faculty of Science, University of Hong Kong, Pokfulam Road, Hong Kong, China

Received 20 November 2006; received in revised form 23 April 2007; accepted 24 April 2007

Abstract

Recent millimeter-wave and infrared spectroscopic observations have identified a large number of organic molecules through their rotational and vibrational transitions. In particular, the detections of the stretching and bending modes of aliphatic and aromatic compounds have revealed a continuous synthesis of organic materials at the late stages of stellar evolution. High resolution imaging observations in the submillimeter (e.g., *SMA*) and in the mid-infrared (e.g., *Gemini*) have made possible the mapping of the distribution of these compounds, allowing us to infer the history of circumstellar chemistry. In this paper, we present some of the recent spectroscopic and imaging observations of the circumstellar envelopes of evolved stars and discuss a scenario of chemical evolution including the possible role of photochemistry in the late stages of stellar evolution.

© 2007 Published by Elsevier Ltd on behalf of COSPAR.

Keywords: Planetary nebulae; Interstellar molecules; Organic compounds; Infrared astronomy

1. Introduction

It is now widely recognized that the late stages of evolution from the end of the asymptotic giant branch (AGB) to proto-planetary nebulae (PPN), to planetary nebulae (PN) represent an active phase of molecular synthesis. Through the technique of mm and submm spectroscopy, the rotational transitions of over 60 molecules have been detected. These include inorganics (CO, SiO, SiS, NH₃, AlCl), organics (C₂H₂, CH₄, H₂CO, CH₃CN), radicals (CN, C₂H, C₃, HCO⁺), cyclic molecules (C₃H₂), cyanopolyynes (HCN, HC₃N, ..., HC₉N), methycyanopolyynes (CH₃C_{2n+1}H), polyacetylenic radicals (C_nH), polyacetylenes (H-(C≡C)_n-H), and pure carbon chains (C_n). With the technique of infrared spectroscopy, the vibrational stretching and bending modes of both inorganic minerals and organic carbonaceous compounds have been observed. Of particular significance is the detection of aromatic and aliphatic compounds and the demonstration that rapid chemical synthesis of complex organic compounds is

possible in the low-density circumstellar conditions over time scales as short as a few hundred years (Kwok, 2004).

However, most of the millimeter and submillimeter observations of molecules in the past have been obtained with single-dish telescopes. While we can trace the chemical evolution by observing objects in different stages of evolution, it would be desirable if the spatial distribution of the gas-phase molecules and the solids can be mapped directly. A detailed map of the emission region of different species can be used to trace the chemical synthesis history and therefore test our chemical models.

2. High angular resolution infrared and submm imaging

Advances in adaptive optics technique in ground-based infrared telescopes have led to the possibility of diffraction-limited imaging in the mid-infrared. For example, the Thermal Region Camera Spectrograph (T-ReCS) and the Michelle imager and spectrometer at the 8-m *Gemini south telescope* can routinely achieve 0.4 in. resolution at 10 μm, and 0.1 in. resolution after deconvolution. These resolutions are comparable to the *Hubble Space Telescope (HST)* spatial resolutions in the optical and therefore

E-mail address: sunkwok@hku.hk

allow direct comparison between the optical and mid-IR images.

Fig. 1 shows the *Gemini* mid-IR images of the PPN IRAS 17441–2411. This is a bipolar reflection nebula with the two optical lobes separated by a dark lane, probably due to obscuration by a dust torus (Su et al., 1998). In this *Gemini* image, the dust torus is clearly detected in emission, but its orientation is not perpendicular to the optical bipolar lobes. The angular separation between the infrared disk and the dark lane in the optical image is estimated to be 23° . Such a misalignment may be related to the phenomenon of multiple bipolar lobes in PN, examples of which include NGC 6881 (Kwok and Su, 2005) and NGC 2440 (López et al., 1998). Although the origin of multiple lobes is not known, precession has been suggested to be one of the possible causes (Miranda et al., 1999).

Another example of distribution of dust in a bipolar reflection nebula is Hen 3-401. By subtracting the $11.38\ \mu\text{m}$ map from the $11.66\ \mu\text{m}$ map, we can obtain the distribution of the aromatic infrared band (AIB) emission. There is some suggestive evidence from the map that the AIB carriers are synthesized in discrete shells where the fast outflow interacts with pre-existing slower moving gas (Muthumariappan et al., 2006).

In the mm- and submm regions, high-angular resolution images can be obtained through the technique of aperture synthesis. In particular, the recently commissioned *Submillimeter Array (SMA)* on Mauna Kea is capable of achieving an angular resolution of 0.4 in. at 230 GHz, and 0.3 in. at 345 GHz. For example, a detached shell has been detected in the CO $J=2-1$ image of the bright, carbon star R Scl. With a diameter of 30 in. and an observed expansion velocity of $15.9\ \text{km s}^{-1}$, the shell was ejected 1600 (D/360 pc) years ago.

Fig. 2 shows CO $J=3-2$ emission in grey scale, tracing the molecular envelope of the young PN NGC 7027. Since the spectral energy distribution of NGC 7027 is

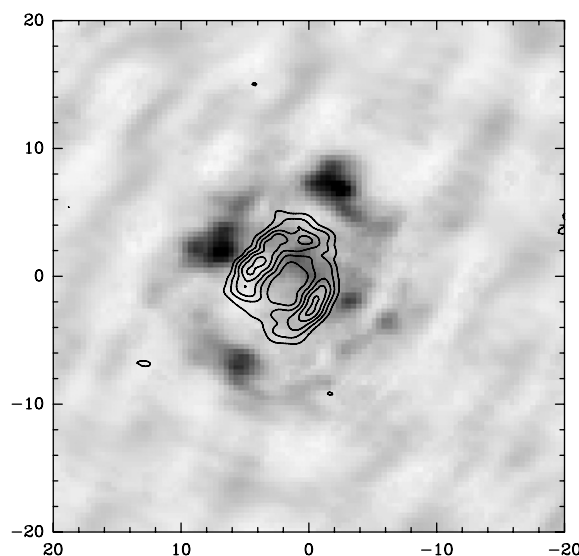


Fig. 2. The 345 GHz continuum map of NGC 7027 (shown as contours in intervals of 15 mJy/beam) compared to the CO $J=3-2$ emission (shown in grey scale). The beam is 1.71×0.85 .

well covered in the far infrared, submm, and radio regions by photometric observations, the dust and free-free emission components can be readily separated. The continuum emission at 345 GHz (shown in contours) is primarily due to free-free emission. We can see that the molecular envelope (shown in grey scale) lies outside the ionized region.

From the *SMA* CO $J=3-2$ image of the PPN IRAS 07134 + 1005 shows a clear detached shell, similar to the mid-infrared image of the object observed by Kwok et al. (2002). From the kinematic information derived from the CO map, we can determine that the southeast side of the molecular torus is tilted away from us.

Fig. 3 shows that the molecular outflow in the PN NGC 2440 has a bipolar form, and is aligned along the same axis

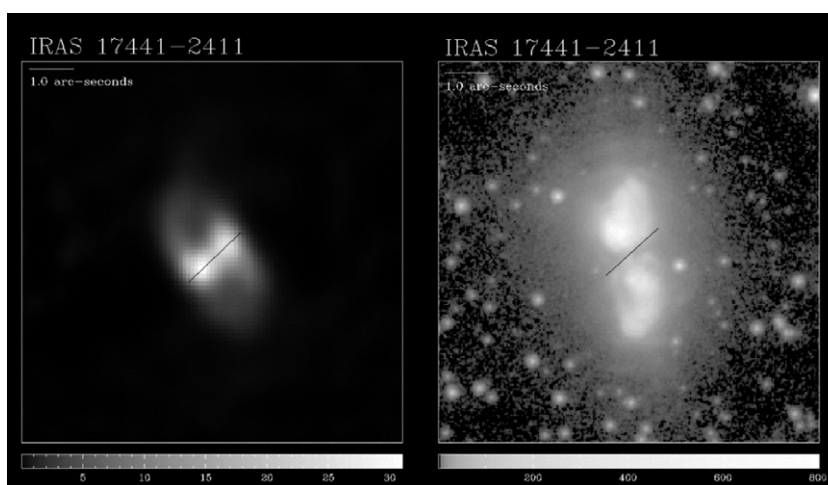


Fig. 1. *Gemini* T-ReCs $11.7\ \mu\text{m}$ image of PPN IRAS 17441-2411 (left). The orientation of the infrared disk is overlaid on the optical I band *HST* image (right) as a solid line. The *Gemini* image is on a linear scale with the grey scale in units of Jy/sq. arcsec. The *HST* image is in logarithmic units of raw counts.

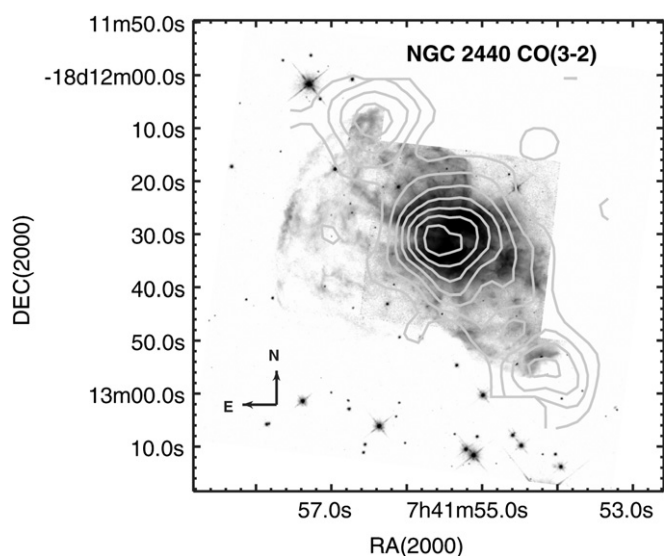


Fig. 3. The *JCMT* CO $J=3-2$ map (in contours) is overlaid with the *HST* WFPC image of NGC 2440. The velocity interval of CO emission is $35-55 \text{ km s}^{-1}$. The lowest contour and the contour interval are both 0.63 K km s^{-1} .

as the primary optical bipolar lobes of this multipolar object (Wang et al., submitted for publication).

In the example of IRAS 17441–2411, we see that mid-infrared imaging can show that optical imaging does not necessarily represent the complete picture of the morphology of PPN, and mapping of the dust distribution is necessary to understand the dynamical origin of the observed morphologies. For Hen 3-401, it is shown that through narrow-band imaging in the infrared, the distribution of different chemical species can be mapped and this serves as useful constraints of chemical models. In AGB stars such as R Scl, the circumstellar material is predominantly neutral, and molecular imaging can probe dynamical processes, such as the formation of detached shells. In PPN, where disks or torus are widely believed to be collimating agents of the bipolar flows, high-resolution molecular and dust imaging will be instrumental in determining the geometry of the disks and torus involved. Planetary nebulae (which NGC 7027 is a good example) are complex systems consisting of ionized, molecular, and solid-state components, and comparisons between optical, infrared and sub-mm images are necessary to discern the radiative and dynamical relationship between the three components. For PN with a complex morphology, such as the multipolar NGC 2440, molecular mapping provides an extra tool to trace the mass distribution in the object.

3. Advantages of circumstellar chemistry

In comparison to interstellar clouds, there are many advantages of using circumstellar envelopes to study the process of chemical synthesis. First, there is only one single energy source – the central star, whose temperature and luminosity are well known. The envelope often has a

well-defined symmetry, making the geometry of the system simple. By using molecular lines and infrared continuum radiation as probes, the physical conditions of the envelope such as density, temperature, and radiation background are well determined. Most importantly, the chemical reaction times are constrained by the dynamical and stellar evolution times, which are $\sim 10^4$ years for AGB stars, 10^3 years for PPN, and 10^4 years for PN. These time scales give us a precise knowledge of the time needed to form one species from another. These allow the development of chemical models that can be rigorously tested by observations.

4. Chemical evolution

Since the aromatic infrared emission features first emerge in the PPN phase, what are the steps leading to the formation of ring molecules? Acetylene (C_2H_2), believed to be the first building block of benzene, is commonly detected in evolved carbon stars through its ν_5 fundamental band at $13.7 \mu\text{m}$. Polymerization of C_2H_2 leads to the formation of diacetylene (C_4H_2) and triacetylene (C_6H_2) in PPN (Fig. 4), cumulating in the formation of benzene (Cernicharo et al., 2001).

In PPN, the 3.4 and $6.9 \mu\text{m}$ aliphatic emission features are as strong as the 3.3 , 6.2 , 7.7 , and $11.3 \mu\text{m}$ aromatic emission features. When the star evolves to the PN stage, the aromatic features become dominant. Fig. 5 shows the spectrum of the young PN IRAS 21282 + 5050 where the $3.4 \mu\text{m}$ aliphatic features can still be clearly seen, but are much weaker than the $3.3 \mu\text{m}$ aromatic feature. A feature at $3.56 \mu\text{m}$ could be due to the aldehyde C–H stretch. If this is true, then the detection of an oxygen-containing compound is of high significance.

The gradual weakening of the 3.4 and $6.9 \mu\text{m}$ emission features from PPN to PN suggests a change from aliphatic to aromatic structures. This could be the result of photochemistry where the onset of UV radiation modifies the aliphatic side groups through isomerizations, bond

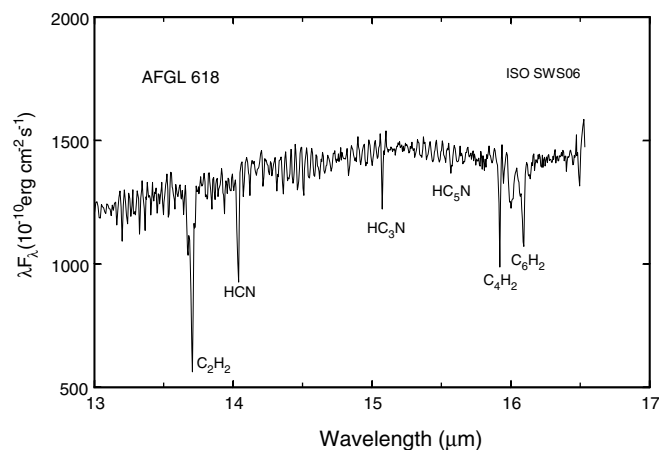


Fig. 4. *ISO* SWS06 spectrum of the PPN AFGL 618 showing absorption features of acetylene, diacetylene, and triacetylene, as well as cyanopolynes (HCN, HC_3N , and HC_5N).

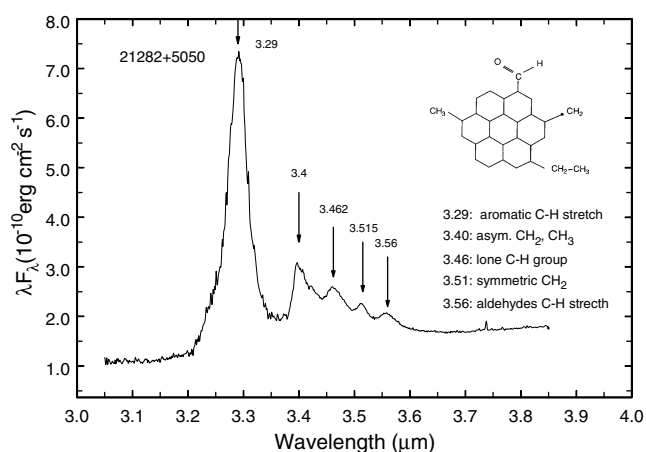


Fig. 5. The spectrum of IRAS 21282 + 5050 taken with the NIRSPEC instrument at Keck Observatory showing the stretching modes of CH_2 and CH_3 sidegroups, as well as the 3.56 μm feature due to aldehydes (Hrivnak et al., 2007).

migrations, cyclization and ring closures and transform them into ring systems (Kwok et al., 2001). Hydrogen loss can also result in fully aromatic rings that are more stable than alkanes or alkenes. Evidence for such H loss can also be found in the weakening of the 12.1, 12.4, and 13.3 μm features and the strengthening of the 11.3 μm feature from PPN to PN (Kwok et al., 1999).

The above scenario of chemical evolution is based on spectroscopic observations of objects in consecutive phases (AGB, PPN, PN) of stellar evolution. In order to test and confirm this chemical model, imaging information is necessary. For example, the spatial distribution of the 3.4 μm aliphatic features in PPN can provide very useful information (Goto et al., 2007). The post-AGB phase of evolution is also a period rich in dynamical activities where a collimated fast outflow transforms the spherical AGB envelope into a bipolar (and sometimes multipolar) PN. To what extent are the chemical processes related to these dynamical activities, in addition to the changing nature of the background radiation? These are questions that need further exploration.

5. Future outlook

We have learned that the circumstellar environment is an ideal laboratory to study the synthesis and chemical evolution of molecules and solid-state compounds. Since these compounds are ejected into the interstellar medium, evolved stars probably play an important role in the chemical enrichment of the Galaxy, and possibly the early solar system. Future instruments such as *SOFIA*, *Herschel* and *ALMA* will have the sensitivity and angular resolution to map out the distribution of different molecular species, and therefore will be able to trace the time-resolved chemical channels for the formation of these species. In planetary nebulae, we can employ different techniques to map the distribution of the ionized gas (e.g., through

recombination lines, collisionally excited lines, and free-free continuum emission), atomic neutral gas (through fine-structure lines), molecular gas (through rotational and vibrational transitions), and the solid-state components (through mid- and far-infrared emissions) and be able to achieve a better understanding of the ionization, excitation, radiative coupling, and dynamical interactions between these components.

Acknowledgements

The works on infrared imaging are done in collaboration with Kevin Volk. The submm imaging work is done in collaboration with Dinh Van Trung, Sebastien Muller, T. Hasegawa and other members of the evolved stars group at *ASIAA*. The infrared spectroscopy work is done in collaboration with Bruce J. Hrivnak and T.R. Geballe. S.K. acknowledges research support from the University of Hong Kong, the Natural Science and Engineering Research Council of Canada, Canada Council for the Arts, the National Science Council of Taiwan, and the Academia Sinica over the periods these works were carried out.

References

- Cernicharo, J., Heras, A.M., Tielens, A.G.G.M., Pardo, J.R., Herpin, F., Guélin, M., Waters, L.B.F.M. Infrared space observatory's discovery of C_4H_2 , C_6H_2 , and benzene in CRL 618. *Astrophys. J.* 546, L123–L126, 2001.
- Goto, M. et al. Diffraction-limited 3 μm spectroscopy of IRAS 04296 + 3429 and IRAS 05341 + 0852: spatial extent of hydrocarbon dust emission and dust evolutionary Sequence. *Astrophys. J.* 662, 389–394, 2007.
- Hrivnak, B.J., Geballe, T.R., Kwok, S. A study of the 3.4 μm emission in proto-planetary nebulae. *Astrophys. J.* 662, 1059–1066, 2007.
- Kwok, S. The synthesis of organic and inorganic compounds in evolved stars. *Nature* 430, 985–991, 2004.
- Kwok, S., Su, K.Y.L. Discovery of multiple coaxial rings in the quadrupolar planetary nebula NGC 6881. *Astrophys. J.* 635, L49–L52, 2005.
- Kwok, S., Volk, K., Bernath, P. On the origin of infrared plateau features in proto-planetary nebulae. *Astrophys. J.* 554, L87–L90, 2001.
- Kwok, S., Volk, K., Hrivnak, B.J. Subarcsecond mid-infrared imaging of two post-AGB 21- μm sources. *Astrophys. J.* 573, 720–727, 2002.
- Kwok, S., Volk, K., Hrivnak, B.J. Chemical evolution of carbonaceous materials in the last stages of stellar evolution. *Astr. Astrophys.* 350, L35–L38, 1999.
- López, J.A., Meaburn, J., Bryce, M., Holloway, A.J. The morphology and kinematics of the complex polypolar planetary nebula NGC 2440. *Astrophys. J.* 493, 803–810, 1998.
- Miranda, L.F., Guerrero, M., Torrelles, J.M. Multiwavelength imaging and long-slit spectroscopy of the planetary nebula NGC 6884: the discovery of a fast processing, bipolar collimated outflow. *Astron. J.* 117, 1421–1432, 1999.
- Muthumariappan, C., Kwok, S., Volk, K. Sub-arcsec mid-IR imaging of dust in the bipolar nebula Hen 3-401. *Astrophys. J.* 640, 353–359, 2006.
- Su, K.Y.L., Volk, K., Kwok, S., Hrivnak, B.J. Hubble Space Telescope imaging of IRAS 17441-211: a case study of a bipolar nebula with a circumstellar disk. *Astrophys. J.* 508, 744–751, 1998.
- Wang, M.-Y., Hasegawa, T.I., Kwok, S. The detection of a molecular bipolar outflow in the multipolar planetary nebula NGC 2440. *Astrophys. J.*, submitted for publication.